Compressed Sensing ISAR 3D Imaging Methods Based on OMP Algorithm

Jingcheng Zhao, Zongkai Yang, and Shaozhu Gu(✉)

School of Electronics and Information Engineering,
Beijing University of Aeronautics and Astronautics, Beijing 100191, China
gushaozhu@126.com

Abstract. In the application of three-dimensional imaging inverse synthetic aperture radar, the existing matching tracking-based compression tracking reconstruction algorithm has many problems, such as large computer storage and low computational efficiency. Based on the Orthogonal Matching Pursuit (OMP) algorithm, this paper proposes a dimensionality-compressive sensing reconstruction method Kron OMP based on the sparseness of the Inverse-Synthetic-Aperture-Radar (ISAR) target and the three-dimensional separability of the perceptual matrix. Firstly, a three-dimensional ISAR imaging model is established, and the Kronecker product expression method is used to split the perceptual matrix and transform the 3D reconstruction into a two-dimensional reconstruction problem. Comparing the time and memory consumption of the algorithm, the Kron OMP algorithm reduces the computer memory requirements of the perceptual matrix by more than 95% during the reconstruction process and reduces the computation time by more than 90%. Simulation experiments verify the effectiveness of the algorithm.

Keywords: Compressed sensing · ISAR · OMP · Three-dimensional imaging · Signal reconstruction

1 Introduction

Compared to optical imaging, microwave imaging offers all-weather, all-day, long-range detection and high resolution. Inverse-Synthetic-Aperture-Radar (ISAR) is a high-resolution imaging system [1]. A high resolution of the range is achieved by transmitting a wideband signal, and a high resolution is achieved in the azimuth and pitch directions by inversely synthesizing the aperture. For turntable measurement systems, large-scale sampling of azimuth and pitch directions will consume a large amount of test time, while dense sampling of wideband signals will place higher demands on hardware devices. In 2006, Candes et al. used mathematical derivation to prove that the original signal can be reconstructed by partial Fourier transform coefficients, which lays the theoretical foundation of Compressed Sensing (CS) [2]. Based on these results, Donoho formally proposed the concept of compressed sensing theory and related theoretical framework [3]. The compressed sensing method utilizes the sparseness of the signal, and reconstructs the original signal based on the amount of measured data of the signal is much smaller than that of the traditional sampling

S. Han et al. (Eds.): AICON 2019, LNICST 286, pp. 279–292, 2019.
https://doi.org/10.1007/978-3-030-22968-9_25

method, which breaks through the limitation of the Shannon-Nyquist sampling theorem. After the theory of compressed sensing, Baraniuk first proposed the application of compressed sensing theory to radar imaging in 2007 [4]. Since then, the application of compressed sensing to radar imaging has received extensive attention from scholars at home and abroad, and has achieved a series of research results [5–8]. At present, typical reconstruction algorithms can be divided into three categories: (1) Convex optimization algorithm, which is solved by transforming non-convex problems into convex problems. This type of algorithm requires less measurement and high reconstruction accuracy, but the computational complexity is high and the efficiency is low. (2) Combining algorithms to reconstruct signals by packet detection. Although this type of algorithm is faster, it requires a special structure to be included in the measurement object and the observation matrix is sparse. (3) The greedy algorithm approximates the original signal by selecting the atom most relevant to the original signal. This type of algorithm has low computational complexity and high efficiency, and has become the mainstream algorithm [9]. OMP algorithm is one of the most representative greedy algorithms. It has the advantages of simple implementation, stable performance and low computational complexity. It has been widely studied by scholars. However, the compressed sensing algorithm reduces the sampling rate of the system, improves the imaging quality and reduces the amount of sampled data, while increasing the requirements of the algorithm for computer memory during the reconstruction process. For the OMP reconstruction process in the 3D ISAR scenario, the measurement matrix can easily reach hundreds of GB, and the computer memory cannot store such huge data explicitly. Therefore, it is urgent to study a new method to solve this problem.

At present, the research on the field of ISAR three-dimensional imaging for compressed sensing mainly includes the following contents. In [8], the theory of compressed sensing is applied to the reconstruction process of InISAR two-dimensional image, and then multiple two-dimensional images are synthesized into three-dimensional images by conventional restoration method. However, this single processing method is insufficient, and the premise of using this method is different coherence. The antennas have the same sparse support. In [10], InISAR imaging is proposed as a kind of multi-channel ISAR imaging, and combined with sparsity constraints to improve the accuracy of target height estimation. In [11], under the premise of small target size, the perceptual matrix is set to a one-dimensional long vector by means of compressed sensing method, and the target three-dimensional image is reconstructed by OMP method. Reduced sampling rate and reduced sampling time, but increased the need for memory. In [12], based on the 3-dimensional decomposable property of the echo matrix, a dimensionality reduction method is proposed to develop the three-dimensional ISAR problem into two-dimensional calculation. The method uses 2DSL0 method to process the two-dimensional data to reduce the storage capacity. The computational efficiency is improved, but the 2DSL0 method has the problems of low imaging dynamic range and many false scattering points, and this method has high requirements for parameter selection. In [13], a two-dimensional joint super-resolution method is proposed. Based on the echo signal of pulse compression, an imaging algorithm suitable for three-dimensional is proposed, but the algorithm is mainly used for MIMO imaging with low resolution. In [14], the

scene segmentation method is used to divide the large scene into several small scenes for imaging separately, and finally the results are stacked in order to obtain the ISAR three-dimensional image in the large scene. The algorithm improves the calculation speed while solving the ISAR three-dimensional imaging problem in large scenes, but it has strict requirements for scene segmentation. Once the scattering point is at the edge of the sub-scene, it will generate a strong reconstruction of nearby sub-scene interference.

In this paper, when the matching tracking algorithm is applied in 3D ISAR imaging, the echo is complex, the data volume is large, and the computational complexity is high, which makes it difficult to calculate. According to the 3D separability of the radar echo sparse dictionary and the compressed measurement matrix, the Kronecker product is utilized. The way to expand the 3D signal to 2D, using Kron OMP processing method, the perceptual matrix of the reconstruction process reduces the computer memory requirements by more than 95%, and shortens the calculation time by 90% the above. The remainder of this paper is organized as follows: Part 2 derives the three-dimensional representation model of the radar echo signal, and Part 3 introduces the process of three-dimensional model expansion to two-dimensional, and introduces the solution to the three-dimensional ISAR compression-aware Kron OMP algorithm. The fourth part is The MATLAB simulation results of simple targets, the fifth part is the FEKO simulation results of complex targets, and the sixth part is the summary of the article.

2 3D ISAR Imaging Model Based on Compressed Sensing

In this paper, the three-dimensional imaging method optimization of the turntable target is studied. For the ISAR imaging of the moving target, after motion compensation, the model can be equivalent to the three-dimensional turntable model. Therefore, this research has universality for ISAR imaging. The schematic diagram of the relationship between radar and turntable targets is as follows:

The target coordinate system X-Y-Z is established with the target center as the coordinate origin, which rotates with the target. Another coordinate system u-v-n is established along the direction of the radar, which is fixed and does not rotate with the target. Radar can get high resolution in range direction by transmitting broadband signals. As shown in Fig. 1, target rotates around n axis with azimuth angle θ and rotates around axis v with pitch angle φ. The azimuth and pitch inverse synthetic aperture scans are used to obtain high resolution in these two directions. The distance between the radar and the turntable target center is R_0. At the moment t, the projection of a point P(X, Y, Z) on the target along the u axis in the u-v-n can be expressed as:

$$R(\mathrm{t}) = R_0 + x\cos\theta(t)\cos\varphi(t) - y\sin\theta(t)\cos\varphi(t) + \mathrm{z}\sin\varphi(t) \tag{1}$$

Where, φ(t) represents the change of the angle versus time in pitch direction. θ(t) indicates the change of the angle versus time in azimuth direction. Using stepped frequency radar signal, the initial frequency is set to f_0, the frequency step length is Δf, the frequency bandwidth is B = (N − 1)Δf, and the stepped frequency number is N.

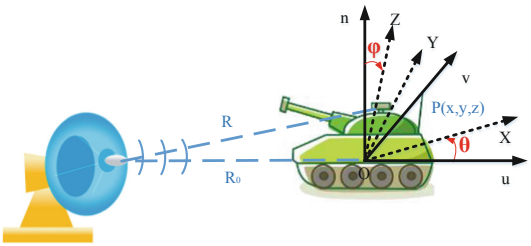

Fig. 1. Relative position between radar and the target on the turntable

Considering the far-field and small-angle observation conditions, after mixing the echo data, the echo data of the m-azimuth, the l-elevation and the n-sampling frequency points can be expressed as follows:

$$\begin{aligned} s(f_n, \theta_m, \varphi_l) &= \sum_{i=1}^{I} \sigma_i \exp\left(-\mathrm{j}\frac{4\pi f_n R}{c}\right) \\ &= \sum_{i=1}^{I} \sigma_i \exp\left(-\mathrm{j}\frac{4\pi f_n}{c}\left(x_i \cos\theta_m \cos\varphi_l - y_i \sin\theta_m \cos\varphi_l + z_i \sin\varphi_l\right)\right) \\ &= \sum_{i=1}^{I} \sigma_i \exp\left(-\mathrm{j}\frac{4\pi f_n}{c}\left(x_i - y_i + z_i\varphi_l\right)\right) \end{aligned} \tag{2}$$

Where σi is the scattering coefficient of the *i*th (i = 1,2, …, I) scattering point in the target space. The frequency of the nth pulse is $f_n = f_0 + (n-1)\Delta f$, n = 1,2, …, N. The azimuth and pitch observation angles are discretized. The azimuth angle is $\theta_m = (m-1)\Delta\theta$, where $\Delta\theta$ is azimuth angle sampling interval and the pitch angle is $\varphi_l = (l-1)\ \Delta\varphi$, l = 1,2, …, L, where Δφ is pitch angle sampling interval. Three-dimensional scattering distribution $\sigma = [\sigma_{p,q,k}]$ P × Q × K can be obtained by discrete sampling of the scattering rate function of the object.

$$\begin{cases} x_p = p\Delta x, p = 1, 2, \ldots, P \\ y_q = q\Delta y, q = 1, 2, \ldots, Q \\ x_k = k\Delta z, k = 1, 2, \ldots, K \end{cases} \tag{3}$$

Where $\Delta x = c/2(P-1)\Delta f$, $\Delta y = \lambda_0/2(Q-1)\Delta\theta$ and $\Delta z = \lambda_0/2(K-1)\Delta\varphi$ respectively represent the resolution of the three dimensions. $P = E_1N$, $Q = E_2M$, $K = E_2L$. E_1, E_2, E_3 are the super-resolution multiples of the three directions, respectively. In case $E_1 = E_2 = E_3 = 1$, the imaging resolution is consistent with the traditional method. $\lambda_0 = c/f_0$ is the initial signal wavelength, in general $\lambda_0 \approx \lambda_n$, therefore, Eq. (2) can be written as:

$$s(n,m,l) = \sum_{P=0}^{P-1}\sum_{Q=0}^{Q-1}\sum_{K=0}^{K-1}\sigma(p,q,k)exp(-2j\pi\frac{p(n-1)}{p}) \exp(-2j\pi\frac{p(n-1)}{p})exp(-2j\pi\frac{p(n-1)}{p}) \tag{4}$$

When the scattering point distribution σ = [σp, q, k]P × Q × K is sparse, it can be solved by compressed sensing. Write the formula in the form of a matrix or a vector. S = [yn, m, l] N × M × L represents the 3D observation echo matrix and change the matrix into a vector:

$$\mathrm{S_{NML\times 1}} = [\mathrm{s(1,1,1)} \ldots \mathrm{s(N,1,1)} \ldots \mathrm{S(N,M,1)} \ldots \mathrm{S(N,M,L)}]^{\mathrm{T}} \tag{5}$$

At the same time, the target scattering point distribution is also changed into a vector:

$$\sigma_{\mathrm{PQK}\times 1} = [\sigma(1,1,1) \ldots \sigma(\mathrm{P},1,1) \ldots \sigma(\mathrm{P},\mathrm{Q},1) \ldots \sigma(\mathrm{P},\mathrm{Q},\mathrm{K})]^{\mathrm{T}} \tag{6}$$

$\varphi_r = [exp(-2j\pi p(n-1)/\mathrm{P})]_{\mathrm{N}\times\mathrm{P}}$, $\varphi_c = [exp(-2j\pi p(m-1)/\mathrm{P})]_{\mathrm{M}\times\mathrm{Q}}$ and $\varphi_v = [exp(-2j\pi p(l-1)/\mathrm{P})]_{\mathrm{L}\times\mathrm{K}}$ are respectively Fourier dictionaries in distance direction, azimuth direction and pitch direction. Based on the above formula, the relationship between the observed data and the imaging space can be obtained as

$$S_{NML} \times 1 = (\varphi_v \otimes \varphi_c \otimes \varphi r)\sigma_{PQK} \times 1 = \varphi_{NML\times PQK}\sigma_{PQK\times 1} \tag{7}$$

Where, ⊗ represents the Kronecker operator, $\varphi_{\mathrm{NML}\times\mathrm{PQK}}$ is the sensing matrix. Formula (7) is the Kronecker decomposition for the three-dimensional ISAR imaging. The compressed sensing can recover the original signal with a small number of sampling points under the premise of target sparsity. The observation matrices in the three directions of distance, azimuth and elevation are respectively $\gamma_{\mathrm{r}}, \gamma_{\mathrm{c}}$ and γ_{v} with the sizes $\mathrm{G_{1\times N}}, \mathrm{G_{2\times M}}$ and $\mathrm{G_{3\times L}}$. The imaging formula by compressed sensing can be expressed as:

$$u_{\mathrm{G_1G_2G_3}\times 1} = (\gamma_v\varphi_v) \otimes (\gamma_c\varphi_c) \otimes (\gamma_r\varphi_r)\sigma_{\mathrm{PQK}\times 1} = \psi_{\mathrm{G_1G_2G_3}\times\mathrm{PQK}}\sigma_{\mathrm{PQK}\times 1} \tag{8}$$

Among them, $\Theta_v = \gamma_v\varphi_v$, $\Theta_c = \gamma_c\varphi_c$ and $\Theta_r = \gamma_r\varphi_r$ are the compressed sensing dictionary matrix in the pitch direction, the azimuth direction and the distance direction, respectively. $\psi_{\mathrm{G_1G_2G_3}\times\mathrm{PQK}}$ is the global sensing matrix. Therefore, the compressed sensing solution of this problem can be expressed as the following form:

$$\widehat{\sigma} = \min_{\sigma}\|\sigma\|_0, \ \text{s.t.}\|s - \psi s\|_2 \le \varepsilon \tag{9}$$

Where, $\|\cdot\|_p$ means the lp norm.

Compressed sensing algorithm greatly reduces the amount of data needed for measurement, reduces the testing time and improves the testing efficiency. However, the requirement of computational resources is greatly increased in the process of algorithm reconstruction. For example, for a matrix of radar echo data size

61 × 61 × 61, the target space is imaged with 2 times resolution, which means E1 = E2 = E3 = 2, the target space mesh size is equal to 121 × 121 × 121, and the resulting perception matrix size is 226981 × 1771561. Conventional OMP algorithms are difficult to calculate on ordinary computers and small workstations. When the resolution is further increased, the sensing matrix will increase exponentially. The reason for this problem is that the OMP algorithm used to solve the three-dimensional imaging problem in vector, which makes the sensing matrix increase sharply, and it is difficult to express it explicitly in computer memory.

3 Three-Dimensional Reduction Algorithm

In order to solve the problem raised in the second part, this paper improves the OMP algorithm to solve the problem that the matching pursuit compressed sensing method is difficult to calculate in the application of ISAR three-dimensional imaging. The method flow is shown in the following figure (Fig. 2).

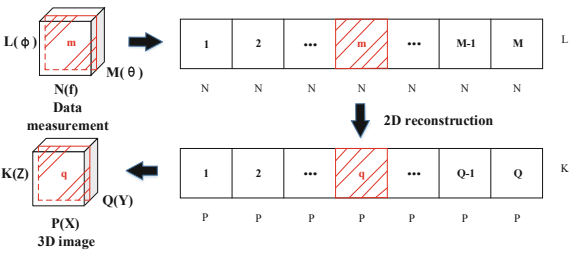

Fig. 2. Kron OMP ISAR 3D imaging flow chart

Firstly, we need to change three-dimensional echo data into two-dimensional form along a certain plane [13]. Because the test space and target space studied in this paper are cubic distribution, the range-pitch slice is chosen to change. In practice, it can be changed in the direction with more test points, and better optimization results can be obtained. Then Kron OMP algorithm is used to solve the two-dimensional reconstruction problem. In the process of solving the problem, the scattering matrix of the target needs to be arranged in two-dimensional form $\widehat{g}_{\mathrm{PQ}\times\mathrm{K}}$. Finally, the two-dimensional scattering coefficient distribution obtained by the solution can be rearranged into three-dimensional. At this point, Eqs. (8) and (9) can be expressed as

$$\mathrm{U}_{\mathrm{G_1G_2G_3}} = (\Theta_c \otimes \Theta_r)\widehat{g}_{\mathrm{PQ}\times\mathrm{K}}\Theta_v^{\mathrm{T}} \tag{10}$$

$$\widehat{g} = \min_g \|g_0\|, \text{s.t.} \left\|U - (\Theta_c \otimes \Theta_r)\widehat{g}_{\mathrm{PQ}\times\mathrm{K}}\Theta_{v2}^{\mathrm{T}}\right\| \leq \varepsilon \tag{11}$$

The details for solving the formula (11) using the Kron OMP algorithm are shown in Table 1. The key of the algorithm is to avoid the explicit storage of the huge vector and to store two dictionary matrices, which greatly reduces the demand for computer memory.

The steps of 3D ISAR imaging algorithm based on OMP are as follows.

Input: $\Theta_v, \Theta_c, \Theta_r$ measurement vector in CS method $u_{G_1G_2G_3\times 1}$, scattering sparsity of target K

Output: 3-D scattering distribution of Target

Kron OMP process steps:

(1) Let $A = \Theta_c \otimes \Theta_r$, $B = \Theta_v$, residual signal vector $r = u_{G_1G_2G_3\times 1}$, index set $\Omega = \emptyset$, empty matrix φ for saving estimation vector, iteration times k = 1;

(2) Find the index ii in sensing matrix ψ, which is the index of the column that has the largest correlation with residual signal vector r. The specific method is to arrange the residual signal vector r into two-dimensional matrix $R_{NM\times K}$. Calculate $y^H r = (\Theta_v \otimes \Theta_c \otimes \Theta_r)^H r = (\Theta_c \otimes \Theta_r)^H R_{NM\times K}\Theta_v^* = A^H R_{NM\times K} B^*$, and record the row number and column number of the maximum;

(3) According to the row and column number acquired in step (2), find the corresponding column vector in $\psi.\omega_k$ = B(:,col) ⊗ A(:,row), update index set $\Omega = \Omega \bigcup \{ii\}$, update the matrix $\varphi = [\varphi, \omega_k]$;

(4) Estimation by least square method $\widehat{\sigma} = \left(\omega_k^H \omega_k\right)^{-1} \omega_k^H r$;

(5) Updating residual signals r = u − $\omega_k \widehat{\sigma}$, update k = k+1;

(6) Determine whether k > K is valid, if it is valid, stop iteration, otherwise, repeat steps (2)–(5);

(7) Rearrange the result $\widehat{\sigma}$ into three dimensions, and output the 3-D scattering distribution of Target.

Through the above algorithm, we can solve the computational difficulty problem of ISAR three-dimensional using compressed sensing. The original method needs to perceive matrix memory O(MNLPQK). After adopting the new method, only O (MNPQ+LK) size data need to be stored, and the demand for memory is reduced by more than 95%.

4 MATLAB Simulation Results

The computer is Windows7 system and the processor is Intel(R) Xeon(R) X5650. The two processors have a clock speed of 2.67 GHz and 2.66 GHz respectively, and the installed memory is 48.0 GB. The MATLAB version is MATLABR2015b, and the radar transmission frequency stepping signal is set. The simulation parameters are shown in Table 1.

Table 1. Simulation parameter setting

Sampling frequency range	10 GHz – 11.5 GHz
Sampling frequency points number	61
Sampling azimuth range	−4.3° ∼ 4.3°
Sampling azimuth points number	61
Sampling pitch angle range	−4.3° ∼ 4.3°
Sampling pitch points number	61

The target consists of 9 scattering points. The echo data is generated according to the point scattering model. The target scattering point distribution and FFT imaging results are shown in Fig. 3. The FFT imaging results are calculated by the ifftn function in MATLAB. It can be seen that the method is imaged. The results have large side lobes and the imaging dynamic range is small. The measured compression ratio d defining the distance, azimuth and pitch directions is N/P, M/Q, L/K, respectively. Assuming that the target scattering point number is known, Fig. 4 shows the CS imaging result of the Kron OMP algorithm in the three-dimensional measurement compression ratio d = 1, where the red circle represents the target point position set during the simulation. The imaging target space uses a super resolution of E1 = E2 = E3 = 2 times. At this time, the perceptual matrix of the original OMP algorithm will reach thousands of GB, and the ordinary workstation cannot explicitly store the matrix data, and thus cannot be calculated. The Kron OMP algorithm can be used to image the target under the parameter by Kronecker multiplication integral solution. The

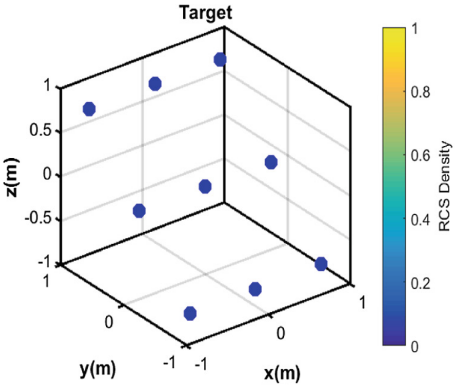

a. Target scattering

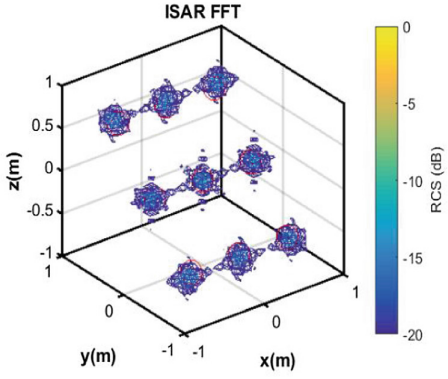

b. FFT imaging result

Fig. 3. Simulated target scattering point and FFT imaging results

specific consumption time and memory comparison are shown in Table 2. Compared with the FFT imaging results, the Kron OMP algorithm has no side lobes and the imaging dynamic range is larger.

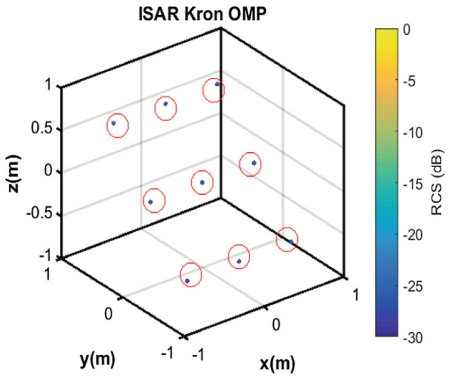

Fig. 4. CS Kron OMP imaging results by simulation when compression ratio d = 1 (Color figure online)

Table 2. Comparison of original OMP and Kron OMP algorithm

Algorithm name	OMP (d = 1)	OMP (d = 3)	Kron OMP (d = 1)	Kron OMP (d = 3)
Time consumption/s	/	6.449	5.860	0.159
Memory consumption/GB	/	9.511	0.812	0.011

Figure 5 shows the CS imaging results of the original OMP algorithm and the Kron OMP algorithm in the three-dimensional measurement compression ratio d = 3, where the red circle represents the target point position set at the time of simulation. The imaging target space adopts super-resolution of E1 = E2 = E3 times. At this time, the time consumed by the sampling and the amount of processed data are greatly reduced, and the memory consumed by the sensing matrix is greatly reduced. Comparing the imaging results of OMP algorithm and Kron OMP algorithm, the improved algorithm imaging results are basically consistent with the original algorithm results, and the original model can be restored better.

Comparing the OMP algorithm and the Kron OMP algorithm in Table 2 with respect to time and memory consumption, the new algorithm can significantly reduce the requirements of the ISAR compression-sensing 3D imaging for hardware memory systems. In this example, the Kron OMP algorithm is used for different data volumes. Computer memory requirements have dropped by more than 95%, and time has also been reduced by more than 90%.

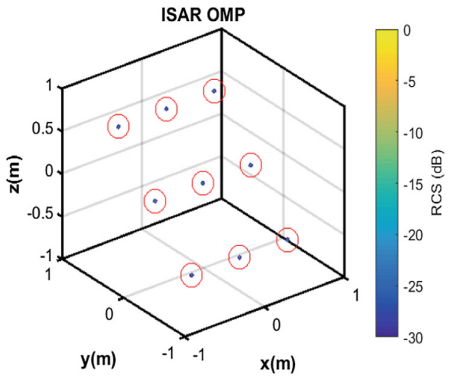

a. OMP imaging results

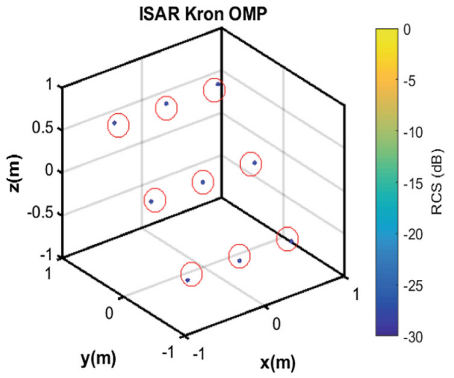

b. Kron OMP imaging results

Fig. 5. CS Kron OMP imaging results by simulation when compression ratio d = 3 (Color figure online)

5 FEKO Simulation Results

This simulation is simulated by the 2017 version of FEKO software. FEKO software is a 3D full-wave electromagnetic simulation software. The simulation parameters are set in Table 2. The target model is shown in Fig. 6, which is a 45° oblique view of the model and a side view. The measured compression ratio d defining the distance, azimuth and pitch directions is N/P, M/Q, L/K, respectively. Set the target sparsity K = 100. Figure 7 shows the 3D imaging of the FFT algorithm. The FFT imaging results are calculated by the ifftn function in MATLAB. It can be seen that the imaging results have large side lobes and imaging. The dynamic range is small. Figure 8 shows the CS imaging results of the Kron OMP algorithm when the compression ratio d = 1 is measured in three dimensions. The imaging target space uses double super resolution. At this time, the perceptual matrix of the original OMP algorithm will reach thousands of GB, and the ordinary workstation cannot explicitly store the matrix data, and thus cannot be calculated. The Kron OMP algorithm can be used to image the

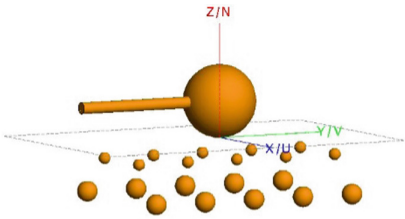

a. Target oblique view

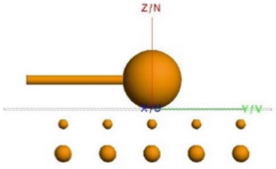

a. Target side view

Fig. 6. Simulation target model

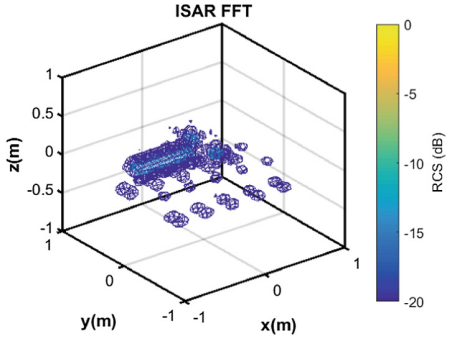

Fig. 7. FFT imaging results by simulation when compression ratio d = 1

target under the parameter by Kronecker multiplication solution. The specific consumption time and memory comparison are shown in Table 3. Compared with the FFT imaging results, the Kron OMP algorithm has no side lobes and the imaging dynamic range is larger.

Figure 9 shows the CS imaging results of the original OMP algorithm and the Kron OMP algorithm when the three-dimensional measurement compression ratio is d = 3. At this time, the time consumed by the sampling and the amount of processed data are greatly reduced, and the memory consumed by the sensing matrix is greatly reduced. Comparing the imaging results of OMP algorithm and Kron OMP algorithm, the improved algorithm imaging results are basically consistent with the original algorithm results, and the original model can be restored well.

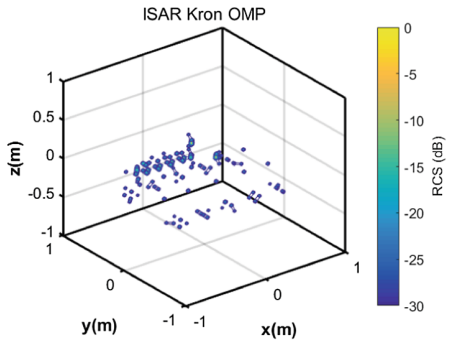

Fig. 8. CS Kron OMP imaging results by simulation when compression ratio d = 1

Table 3. Comparison of original OMP and Kron OMP algorithm

Algorithm name	OMP (d = 1)	OMP (d = 3)	Kron OMP (d = 1)	Kron OMP (d = 3)
Time consumption/s	/	70.982	131.394	4.666
Memory consumption/GB	/	9.511	0.812	0.011

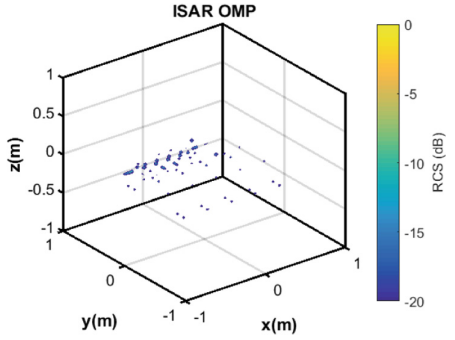

a. OMP imaging results

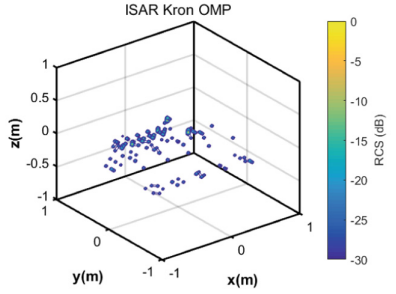

b. Kron OMP imaging results

Fig. 9. CS Kron OMP imaging results by simulation when compression ratio d = 3

Comparing the OMP algorithm and the Kron OMP algorithm in Table 3 with respect to time and memory consumption, the new algorithm can significantly reduce the requirements of the ISAR compression-aware 3D imaging for the hardware memory system. In this example, the Kron OMP algorithm is used for different data volumes. Computer memory requirements have dropped by more than 95%, and time has also been reduced by more than 90%.

6 Conclusion

Compressed sensing method applied to the field of ISAR three-dimensional imaging will bring about the problem of large storage capacity and low computational efficiency. The original OMP algorithm often cannot calculate because the memory consumption of the sensing matrix is too large. In this paper, based on the OPR algorithm, the prior information of sparseness in the spatial domain is used. Based on the OMP algorithm, based on the 3D separability of the perceptual matrix, the Kron OMP method based on the OMP method for ISAR compressed sensing 3D imaging is proposed. The feasibility of the new algorithm is verified by MATLAB simulation and FEKO simulation results. Comparing the time and memory consumption of the two algorithms, the new algorithm reduces the memory requirements of the computer by more than 95% and the time is also more than 90%.

References

1. Fan, H.L.: Research on imaging and Jamming of inverse synthetic aperture radar. University of Electronic Science and Technology of China, Xian (2006)
2. Candes, E.J., Romberg, J., Tao, T.: Robust uncertainty principles: exact signal reconstruction from highly incomplete frequency information (2006)
3. Donoho, D.L.: Compressed sensing. IEEE Trans. Inf. Theory **52**(4), 1289–1306 (2006)
4. Baraniuk, R., Steeghs, P.: Compressive radar imaging. In: Radar Conference (2007)
5. Qiu, W., Zhao, H.Z., Chen, J.J., et al.: High-resolution radar one-dimensional imaging based on smoothed l (0) norm. J. Electron. Inf. Technol. **33**(12), 2869–2874 (2011). Dianzi Yu Xinxi Xuebao
6. Zhang, S.S., Zhang, Y.Q.: Adaptive compressed sensing for high-resolution ISAR imaging. In: Proceedings of EUSAR 2016 11th European Conference on Synthetic Aperture Radar. VDE, pp. 1–4 (2016)
7. Larsson, C.: Compressive sensing methods for radar cross section ISAR measurements. In: 2016 4th International Workshop on Compressed Sensing Theory and its Applications to Radar, Sonar and Remote Sensing (CoSeRa), pp. 237–241 (2016)
8. Zhao, J., Zhang, M.: Performance 3-D ISAR imaging in compact antenna test range via compressed sensing. In: 2017 17th IEEE International Conference on Communication Technology Proceedings, ICCT, 2017 October, pp. 736–740 (2018)
9. Zhu, X.X., Hu, W.H., Guo, B.F.: Overview of ISAR imaging technology based on compressed sensing. Aerodyn. Missile J. (03), 84–89 (2018)
10. Liu, Y., Li, N., Wang, R., Deng, Y.: Achieving high-quality three-dimensional In ISAR imageries of maneuvering target via super-resolution ISAR imaging by exploiting sparseness. IEEE Geosci. Remote Sens. **11**(4), 828–832 (2014)

11. Wei, Q.: Research on multi-dimensional radar imaging method based on compressed sensing. National University of Defense Technology (2014)
12. Qiu, W., Martorella, M., Zhou, J., et al.: Three-dimensional inverse synthetic aperture radar imaging based on compressive sensing. IET Radar Sonar Navig. **9**(4), 411–420 (2015)
13. Wang, D., Ma, X., Chen, A.L., et al.: High-resolution imaging using a wideband MIMO radar system with two distributed arrays. IEEE Trans. Image Process. **19**(5), 1280–1289 (2010)
14. Lü, M., Li, S., Chen, W., et al.: Fast ISAR imaging method based on scene segmentation. J. Syst. Eng. Electron. **28**(6), 1078–1088 (2017)